Microbiological Research 170 (2015) 27–35

Contents lists available at ScienceDirect

Microbiological Research

journal homepage: www.elsevier.com/locate/micres

# Diverse strategies conferring extreme cadmium (Cd) tolerance in the dark septate endophyte (DSE), *Exophiala pisciphila*: Evidence from RNA-seq data

Dake Zhao[a,b,1], Tao Li[a,1], Mi shen[a], Junling Wang[a], Zhiwei Zhao[a,b,*]

[a] *Key Laboratory of Conservation and Utilization for Bioresources and Key Laboratory of Microbial Diversity in Southwest China, Ministry of Education, Yunnan University, Kunming 650091, Yunnan, China*
[b] *School of Agriculture, Yunnan University, Kunming 650091, Yunnan, China*

ARTICLE INFO

*Article history:*
Received 5 June 2014
Received in revised form
10 September 2014
Accepted 17 September 2014
Available online 28 September 2014

*Keywords:*
Dark septate endophytes (DSE)
Transcriptome
Heavy metal tolerance
Cadmium
*Exophiala pisciphila*

ABSTRACT

Dark septate endophytes (DSE) ubiquitously colonize the roots of plants growing in extreme heavy metals (HMs)-contaminated soils. Little is known about the overall molecular response of DSE to excessive HMs. Therefore, RNA-seq was performed through Illumina Hiseq 2000 sequencing based on two cDNA libraries of the DSE strain *Exophiala pisciphila*, cultured under cadmium (Cd)-free and Cd-stressed conditions, and 21,376 unigenes were generated. In total, 575 differentially expressed genes (DEGs) were obtained. Approximately 40% of the DEGs (228 unigenes) were involved in 10 well-known HMs-tolerant pathways, conferring the extreme cadmium (Cd) tolerance of *E. pisciphila*, including metal ion binding and transportation, organic acid metabolism and transportation, reactive oxygen species (ROS) scavenging, redox homeostasis, transcription factors production, sulfate assimilation, DNA repair and cell wall integrity maintenance, etc. Our results indicate that integral tactics associated with the collaboration of extracellular and intracellular mechanisms contribute to the enhanced HMs tolerance of this fungus. This study represents the first investigation of the transcriptome of DSE under Cd stress, and our results provide valuable information for future molecular studies of HMs tolerance in fungi.



## 1. Introduction

Dark septate endophytes (DSE) are characterized by dark pigmented and septate hyphae, constituting a heterogeneous group of root-associated endophytic fungi. These melanocratic fungi have been associated with many plants worldwide (Newsham et al. 2009), and are universally observed under stressed conditions, such as HMs-contaminated environments (Ban et al. 2012; Deram et al. 2008; Ruotsalainen et al. 2007). Previous studies have also shown that DSE inhabited a majority of healthy plants' roots at a mine smelting site with considerably high concentrations of Pb, Zn and Cd (Zhang et al. 2008; Zhou et al. 2013a). DSE even exhibited HMs preference, displaying increased colonization intensities with increasing HMs pollution (Li et al. 2011; Regvar et al. 2011). Despite rigorous challenges associated with excessive HMs, DSE colonization was observed in these harsh environments and indeed showed HMs-tolerance, suggesting these fungi have successfully evolved to adapt to severe HMs-stressed conditions. However, the strategies underlying DSE acclimatization to harsh environments have not been previously discussed, particularly at the molecular level.

Superfluous HMs typically causes serious injuries and even death in most organisms. Exceptional organisms, however, can survive and flourish in HMs-polluted environments in different ways (Bellion et al. 2006; Collin-Hansen et al. 2005; Pócsi 2011). The first step in these defense systems commonly involves extracellular chelating or binding of HMs to cell wall constituents to prevent entrance of HMs. Subsequently, the next step involves a series of intracellular processes, such as complexation and peptide binding, transportation, compartmentalization, ROS scavenging, etc. In addition, for several fungi, such as *Saccharomyces cerevisiae*, positive modulation of the DNA repair pathway would restore HMs-induced injuries (Ruotolo et al. 2008; Serero et al. 2008). However, the powerful global mechanism of DSE HMs tolerance remains unclear.

Cd is one of the most toxic HMs, leading to oxidation, disruptions in sulfhydryl and metal thiolate bonding, alterations in secondary

* Corresponding author at: Cuihu North Road 2#, Key Laboratory of Conservation and Utilization for Bioresources, Yunnan University, Kunming 650091, Yunnan, China. Tel.: +86 871 6503 4799; fax: +86 871 6503 4838.
*E-mail address:* zhaozhw@ynu.edu.cn (Z. Zhao).
[1] These authors contributed equally to this work.

http://dx.doi.org/10.1016/j.micres.2014.09.005
0944-5013/

protein structure and interference with essential metal uptake, transport and metabolism (Bertin and Averbeck 2006). We recently characterized a Cd-tolerant DSE strain (*Exophiala pisciphila*, H93) isolated from the roots of *Arundinella bengalensis*, growing in an old mine smelting site in Yunnan province, southwest China. Surprisingly, H93 showed remarkable Cd tolerance and accumulated over 5% Cd of its dry weight intracellularly, very high tolerance to Pb and Zn was also observed (Zhang et al. 2008). Hence, we speculated that there might be special strategies underlying adaptation to Cd stressed environments for this fungus. To explore these potential tolerance mechanisms, we previously confirmed that the activities of antioxidases, such as superoxide dismutase (SOD) and catalase (CAT), were significantly up-regulated under Cd or Zn stress (Diao et al. 2013; Zhang et al. 2008) and showed that melanin was associated with combating HMs stress (Zhan et al. 2011). In addition, H93 has been shown to enhance maize's tolerance to Pb, Zn and Cd after root colonization (Li et al. 2011). To identify the genes involved in *E. pisciphila* acclimatization to excessive Cd and determine the overall strategies for the survival of this fungus under severe HMs stress, we cultured *E. pisciphila* in Cd-free and Cd-stressed medium, and subsequently performed RNA-seq to investigate the comparative gene expression, functional annotation and enriched metabolic pathways.

## 2. Materials and methods

### 2.1. DSE strain and culture

*E. pisciphila* (H93) was isolated from the roots of *Arundinella bengalensis* (Poaceae), naturally growing in an old mine smelting site in Huize county, Yunnan province, southwest China (Diao et al. 2013; Li et al. 2011; Zhang et al. 2008). The fungus is preserved in the Agricultural Culture Collection Center of China (accession number ACCC32496). H93 was transferred from a PDA slant to Cd-stressed and Cd-free modified Melin-Norkrans (MMN) liquid medium (Zhang et al. 2008) and incubated at $28 \pm 1\,^{\circ}C$, 180 rpm, for 7 days. Each treatment contained 4 replicates respectively. The effective concentration inhibiting growth by 50% ($EC_{50}$ value) is considered to obviously affect the gene expression (Nota et al. 2010; Novais et al. 2012; Zhu et al. 2014). It was calculated in our group by supplementing 0, 25, 50, 100, 200, 400 mg $L^{-1}$ $Cd^{2+}$ into liquid MMN medium with $CdCl_2 \cdot 2.5H_2O$, then, by the method of linear interpolation, $EC_{50}$ value was determined to be 111.2 mg $L^{-1}$ $Cd^{2+}$ (Zhan 2012). To objectively reflect the effect of Cd stress for *E. pisciphila*, $EC_{50}$ value was chosen as the treatment concentration for the Cd-stressed sample.

### 2.2. RNA extraction, quantification and qualification

The hyphae of Cd-free and Cd-stressed samples were collected and intermixed from 4 each replicates. Total RNAs were extracted from the blended hyphae of the two samples using the TRIZOL Kit (Invitrogen, Carlsbad, CA, USA) according to the manufacturer's instructions. The RNA integrity was assessed using the RNA 6000 Nano Assay Kit on the Bioanalyzer 2100 system (Agilent Technologies, CA, USA).

### 2.3. Samples preparation for sequencing

A 3-μg RNA sample was used as input. The RIN (RNA Integrity number) values of the two samples were above 8. The sequenced libraries were generated using TruSeq_RNA_SamplePrep_Guide_15008136_A. The products were purified and quantified using the Agilent High Sensitivity DNA Assay on the Agilent Bioanalyzer 2100 system.

### 2.4. Clustering, sequencing and transcriptome assembly

The clustering of the index-coded samples was performed on the cBot Cluster Generation System using TruSeq PE Cluster Kit v3-cBot-HS (Illumina) according to the manufacturer's instructions. After cluster generation, the preparations were sequenced on the Illumina Hiseq 2000 platform, and 100 bp paired-end reads were produced. Each base was assigning a parameter named sQ value that was indicative of the sequencing quality of bases in all sequenced reads. Low-quality reads was identified as those ones in which the bases with $sQ \leq 5$ account for over 50%. Then, clean reads were obtained after removing low-quality reads by fastQC software (http://www.bioinformatics.babraham.ac.uk/projects/fastqc/). The GC-content of the clean data was calculated. All the downstream analyses were based on clean data. Transcriptome assembly was accomplished based on the read1.fq and read2.fq using Trinity (Grabherr et al. 2011) with min_kmer_cov setting to 2, and all other parameters were set to default.

### 2.5. Quantification of gene expression levels

With the transciptome data from trinity assembly as reference sequences, clean data of the two samples were mapped back onto the reference sequences, then the readcount for each gene was obtained from the mapping results. The process for gene expression levels was estimated by RSEM (Li and Dewey 2011). The RPKM (Reads Per Kilo bases per Million mapped reads) reflected the molar concentration of a transcript and facilitated the transparent comparison of the transcript levels between samples (Mortazavi et al. 2008). We therefore conducted the readcount conversion into RPKM.

### 2.6. Differential expression analysis

Differential expression analysis was performed using the DEG seqR package (Anders and Huber 2011). The *p*-value was adjusted using the *q* value (Storey and Tibshirani 2003). *q* values <0.005 and |log2.Fold_change| > 1 (log2.Fold_change: log2.(Cd-free sample/Cd-treated sample)) were set as the threshold for the significantly differential expression. The obtained DEGs were used to generate the heatmap.

### 2.7. Functional annotation and statistical classification

Functional annotation of the unigenes was predicted based on the highest similarity functions of the unigenes in the following databases: Nr (NCBI non-redundant protein sequences), Nt (NCBI non-redundant nucleotide sequences), Pfam (Protein family), KOG/COG (Clusters of Orthologous Groups of proteins), Swiss-Prot (A manually annotated and reviewed protein sequence database), KO (KEGG Orthology database) and GO (Gene Ontology). Besides, the unigene classification was presented based on the GO database.

### 2.8. DEGs enrichment pathway analysis

For gene expression profiling, we performed an enrichment pathway analysis of the DEGs. The GO enrichment analysis of the DEGs was performed using a GO seq-based Wallenius non-central hyper-geometric distribution (Young et al. 2011), to adjust for gene length bias in the DEGs. Moreover, a KEGG pathway enrichment analysis of the DEGs was also conducted using KOBAS (Mao et al. 2005).

**Table 1**
Statistical summary of the results of the Illumina sequencing and unigene assembly.

| | Cd-free sample | Cd-stressed sample |
|---|---|---|
| Raw reads | 54,424,248 | 52,133,614 |
| Clean reads | 53,095,208 | 50,779,024 |
| Clear bases (G) | 5.30 | 5.08 |
| GC (%) | 50.68 | 50.93 |

### 2.9. Quantitative real-time PCR (qRT-PCR) analysis

To verify the sequencing and expression results, 15 unigenes were selected for confirmation through qRT-PCR analysis. The primers were designed using Primer 5.0 to amplify 80–150 bp regions (Table S1). The qRT-PCR was performed on an Applied Biosystems 7500 Real-Time PCR System (Applied Biosystems, CA, USA) using SYBR Premix Ex Taq (TaKaRa, Japan) according to the manufacturer's instructions. The β-tubulin gene was used as an internal control. The relative quantity was analyzed using the $2^{-\Delta\Delta Ct}$ method of Winer et al. (1999). The obtained data were transformed to log2.Fold_change.

Supplementary table related to this article can be found, in the online version, at http://dx.doi.org/10.1016/j.micres.2014.09.005.

## 3. Results

### 3.1. Sequencing and assembly

A total of 54,424,248 and 52,133,614 raw reads were generated from the control and treated samples, respectively. After cleaning and quality checks, 53,095,208 and 50,779,024 clean reads were obtained, with a data bulk of 5.30 and 5.08 G, and GC figures of 50.68% and 50.93%, for each sample (Table 1). The two libraries were totally assembled into 21,376 non-redundant unigenes. All unigenes were longer than 200 bp, and the longest gene was 15,455 bp and the mean length was 1585 bp. The length distribution of the assembled unigenes is presented in Fig. 1.

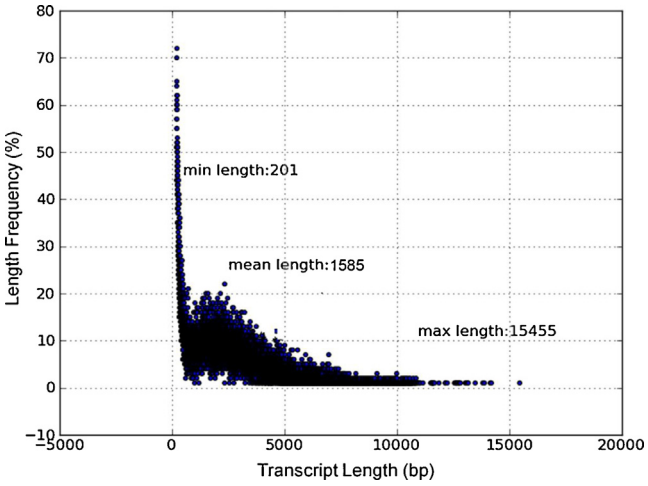


**Fig. 1.** Length distribution of the assembled unigenes of *E. pisciphila*.

### 3.2. Functional annotation of the assembled unigenes of E. pisciphila

The unigenes were annotated based on similarities to the sequences in seven public databases, Nt, Nr, KOG/COG, Pfam, Swiss-sprot, KO and GO. Among the 21,376 unigenes identified, 14,780 genes (69.1%) had at least one hit. Furthermore, 11,924 unique sequences were assigned to one or more ontologies in GO. As demonstrated in Fig. 2, the main biological processes were concerned with biological regulation, cellular processes, establishment of localization, localization, metabolic processes, regulation of biological processes and responses to stimulus groups. The molecular functions were associated with binding, catalytic activity, transporter activity and nucleic acid-binding transcription factor activity. In addition, cells, cell parts, organelles, macrocellular complexes, extracellular regions and organelle parts were the top six largest groups in the category of cellular components.

### 3.3. Gene expression regulated under Cd exposure

The expression of read-mapped genes was analyzed based on the RPKM value for each clean read. We first normalized the read density measurement, and $q$ values <0.005 and |log2.Fold_change| > 1 were set as the threshold to assess the statistical significance of the differential gene expression. Among the 21,376 unigenes identified, approximately 575 differentially expressed genes (DEGs) were detected, including 355 up-regulated genes and 220 down-regulated genes. A heatmap of all 575 DEGs is shown in Fig. 3. The gene expression patterns between the treatments were distinct (Fig. 3). As expected, a majority of DEGs involved in HMs detoxification were listed among the top

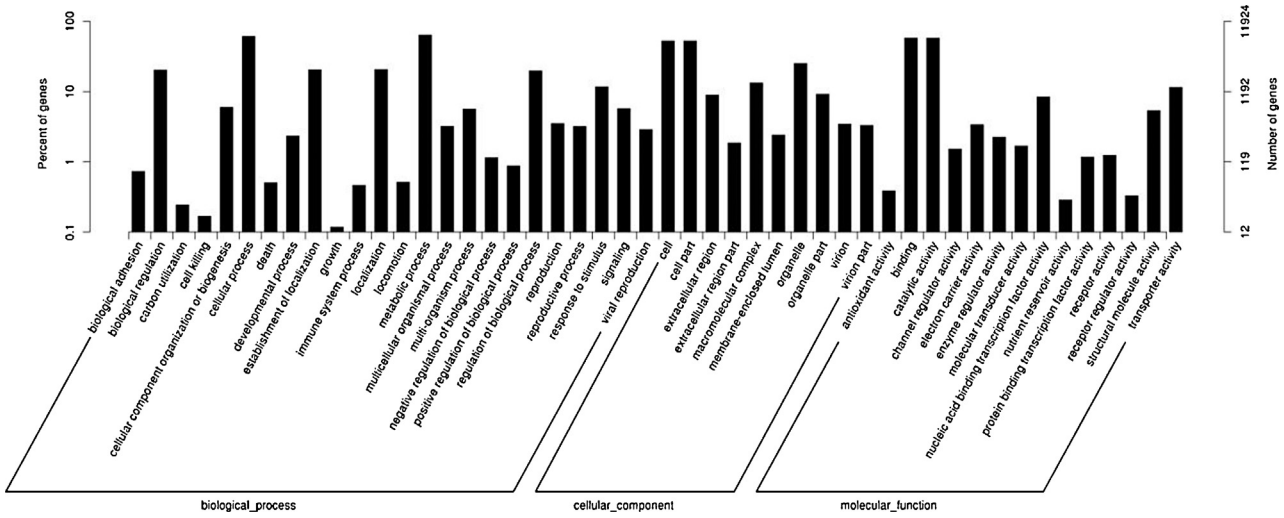


**Fig. 2.** GO categories assigned to unigenes of *E. pisciphila*, including biological processes, cellular components and molecular functions.

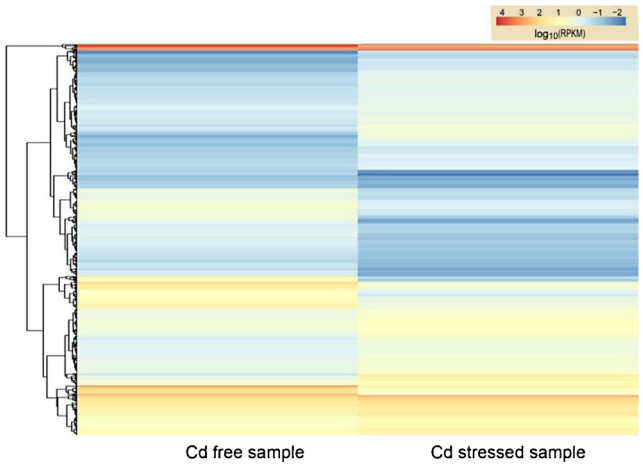


**Fig. 3.** Heatmap of the 575 differentially expressed genes between Cd-free and Cd-stressed samples. The numbers in the upper right bar represent the value of $\log_{10}$ (RPKM). The red color indicates higher expression, and the blue color indicates lower expression. (For interpretation of the references to color in this figure legend, the reader is referred to the web version of the article.)

50 differentially expressed transcripts (Table S2), such as the putative orthologous genes (POGs) of glutathione S-transferase (GST), potassium ion transporters, ACLA_020340, the cation efflux family, the ion-binding family, zinc transporters, etc. One of the glutathione S-transferases (GSTs), which function in sulfate assimilation (Villiers et al. 2011), was identified as the most up-regulated unigene in Cd-stressed *E. pisciphila*.

Supplementary table related to this article can be found, in the online version, at http://dx.doi.org/10.1016/j.micres.2014.09.005.

### 3.4. Identification of Cd-tolerant genes in response to Cd stress

To better assess the biological significance of Cd-modulated DEGs, we enumerated a set of genes associated with HMs tolerance (Bellion et al. 2006; Collin-Hansen et al. 2005; Lagorce et al. 2012; Pócsi 2011; Xu et al. 2012; Zhou et al. 2013b). At least 40% of the DEGs (228 out of 575) were obtained, distributing in/belonging to 10 terms, such as metal binding and transporting, organic acid metabolic processes and transporting, transcription factor, sulfate assimilation, ROS scavenging, cell redox homeostasis, DNA repair, cell redox homeostasis and cell wall metabolic processes (Table S3).

Supplementary table related to this article can be found, in the online version, at http://dx.doi.org/10.1016/j.micres.2014.09.005.

#### 3.4.1. Metal ion binding

Approximately 104 transcripts were involved in metal ion binding for bivalent cation detoxification and homeostasis, such as $Ca^{2+}$, $Fe^{2+}$, $Mn^{2+}$, $Cu^{2+}$, and particularly for $Zn^{2+}$ and non-HMs, such as $K^+$ and $Na^+$. Particularly, 3 genes (comp8373_c0; comp4235_c0; comp12016_c0) were associated with metallothioneins (MTs).

#### 3.4.2. Metal ion transportation

We identified 32 unigenes associated with metal ion transport. In detail, these genes encoded a variety of transporters, such as ATP-binding cassette (ABC) (comp14051_c0; comp10488_c0; comp6936_c0), $K^+$ (comp3213_c0; comp5189_c0; comp10268_c0; comp3165_c0; comp3511_c0; comp11902_c0; comp12921_c0; comp9522_c0; comp10625_c0; comp3208_c0; comp6092_c0; comp10845_c0), $Fe^{2+}$ (comp8165_c0; comp8143_c0; comp6001_c0), $Zn^{2+}$ (comp8143_c0; comp9578_c0; comp6001_c0), $Ca^{2+}$ (comp11611_c0; comp8188_c0) and $Cu^{2+}$ (comp11489_c0; comp15284_c0), $Na^+$ (comp4278_c0; comp8482_c0; comp2369_c0), Zn/Fe (ZIP, comp8143_c0; comp6001_c0), the cation efflux family (comp13051_c0) and other unclear transporters (comp10882_c0; comp13028_c0; comp11233_c1; comp8373_c0). In addition, several $K^+$ ion transporters showed significant up-regulation (8 out of 12), including one gene (comp3213_c0) (Table S2) with a log2.Fold_change of up to 4.4356. $Cu^{2+}$ transporters were also significantly up-regulated, while the genes encoding $Fe^{2+}$, $Zn^{2+}$, $Ca^{2+}$ and $Na^+$ transporters were dramatically down-regulated.

#### 3.4.3. Organic acid metabolic processes and transportation

Approximately 14.1% (63/575) of the DEGs were involved in organic acid metabolic processes and an additional 18 unigenes for organic acid transportation. In particular, we observed that some unigenes were significantly up-regulated, for example, glutamate biosynthetic processes (comp13183_c0; comp14520_c0; comp11910_c0), tricarboxylic acid cycle (comp11969_c0; comp11909_c0; comp14402_c0), valine catabolism (comp3535_c0; comp11529_c0; comp12921_c0), and taurine metabolism (comp6154_c0). However, in several metabolic pathways, such as pyruvate metabolism (comp13319_c0; comp3118_c0) and aromatic metabolism (comp4966_c0; comp13050_c0; comp7124_c0; comp12449_c0) some DEGs were up-regulated and other DEGs were down-regulated after Cd supplementation. In addition, some genes encoded for polyamine transport (comp11587_c0; comp8665_c0), malic acid transport (comp3472_c0; comp12640_c0; comp12031_c0; comp11738_c0) and arginine permease (comp3743_c0). Interestingly, most genes that were differentially expressed in the Cd-stressed treatment were associated with down-regulated fatty acid biogenesis and up-regulated metabolic processes.

#### 3.4.4. Transcription factors (TFs)

We also detected 50 loci encoding TFs, including steA (comp10878_c0), eIF-2C4 (comp8978_c0), IIA(comp10026_c1), Otx1 (comp3511_c0), HCFC1 (comp2984_c0), eIF-5B (comp14992_c0), Tos4 (comp6918_c0), TFIID (comp3140_c0), APSES (comp3745_c0), TFIIB (comp14066_c0), RosA (comp8448_c0), SEF1 (comp11152_c0), DNA-binding transcription factor (comp3165_c0; comp6846_c0; comp8353_c0; comp11518_c0; comp12339_c0; comp12613_c0; comp13050_c0; comp13410_c0), RNA polymerase II transcription cofactor activity (comp3180_c0), C6 transcription factor (comp8448_c0; comp13217_c0), fungal-specific transcription factor (comp3069_c0; comp5562_c0; comp6893_c0; comp9192_c0; comp10140_c0; comp11049_c0; comp11062_c0; comp11586_c0; comp12675_c0; comp16547_c0) and DNA-binding RNA polymerase II transcription factor (comp8416_c0; comp9280_c0; comp9578_c0; comp9822_c0; comp10153_c1; comp10790_c0; comp10886_c0; comp10599_c0; comp11160_c0; comp11902_c0; comp12290_c0; comp13548_c0; comp15509_c0). More than 50% (26 unigenes) of these TFs showed up-regulation.

#### 3.4.5. Sulfate assimilation

Approximately 16 genes showed a close relationship with sulfate assimilation, containing 12 (75%) up-regulated genes, encoding for sulfur transferase (comp11611_c0), sulfate assimilation (comp5516_c0), sulfur compound metabolism (comp12923_c0), ATP-sulfurylase (comp8416_c0), sulfate transporter family (comp12716_c0), sulfate permease C3H7.02 (comp13440_c0), GST (comp3242_c0), carbon-sulfur lyase (comp4130_c0; comp11160_c0; comp11825_c0), phosphoadenylyl-sulfate (PAPS) reductase (comp10824_c0), and iron-sulfur assembly protein 2 (comp13254_c0).

#### 3.4.6. ROS scavenging and cell redox homeostasis

Among the 575 DEGs, 12 loci generated free radical scavengers; for example, the unigenes involved in peroxisomal

**Table 2**
Significantly enriched KEGG terms for DEGs with a threshold of over-represented-*p* value <1 and corrected-*p* value <1 from the comparison of $Cd^{2+}$ stressed and free samples.

| GO accession | Description | Corrected-*p* value | DEG item | BG item |
|---|---|---|---|---|
| GO:0048037 | Cofactor binding | 0.003968 | 76 | 1022 |
| GO:0050662 | Coenzyme binding | 0.069714 | 60 | 852 |
| GO:0016491 | Oxidoreductase activity | 0.069714 | 133 | 2468 |
| GO:0019752 | Carboxylic acid metabolic process | 0.069714 | 63 | 866 |
| GO:0055114 | Oxidation-reduction process | 0.069714 | 121 | 2163 |
| GO:0004601 | Peroxidase activity | 0.10427 | 6 | 25 |
| GO:0006979 | Response to oxidative stress | 0.19233 | 5 | 20 |
| GO:0006631 | Fatty acid metabolic process | 0.50358 | 21 | 247 |
| GO:0006097 | Glyoxylate cycle | 0.51913 | 3 | 6 |
| GO:0046912 | Transferase activity, transferring acyl groups, acyl groups converted into alkyl groupupon transfer | 0.72065 | 4 | 13 |
| GO:0006804 | Peroxidase reaction | 0.7678 | 3 | 11 |
| GO:0016616 | Oxidoreductase activity, acting on the CH-OH group of donors, NAD or NADP as acceptor | 0.84853 | 32 | 452 |

Corrected-*p* value: the *p* value after correcting, a smaller corrected-*p* value indicates more significant differential gene expression. DEG item: the number of DEGs associated with the GO term. BG item: all known genes associated with the GO term.

catalase (comp5960_c0), catalase (comp18838_c0), and Mn superoxide dismutase (SodB) (comp4130_c0) were up-regulated, and the down-regulated genes included POD (peroxidase) reaction (comp11151_c0), POD activity (comp15413_c0), L-ascorbate peroxidase 3 (L-APX 3) (comp8202_c0), cytochrome C peroxidase (CcP) (comp11606_c0), and a DSBA (Dsb, disulfide bond)-like thioredoxin domain (comp3763_c0). Three genes, cell redox homeostasis (comp8548_c0), glutaredoxin (comp12237_c0) and DsbA-like thioredoxin (comp3763_c0) were associated with cell redox homeostasis.

#### 3.4.7. Cell wall integrity maintenance

In cell wall metabolism, four genes encoding chitinase (comp5390_c0; comp6365_c0; comp11037_c0; comp8202_c0) were down-regulated.

#### 3.4.8. DNA repair

Eight genes (comp5516_c0; comp11825_c0; comp11798_c0; comp9654_c0; comp6846_c0; comp9647_c0; comp3089_c0; comp3126_c0) involved in DNA repair were markedly up-regulated.

### 3.5. Enriched pathways detected through GO and KEGG analysis

Among the 575 DEGs, 478 DEGs were annotated in GO, participating in 745 enriched metabolic pathways (over-represented-*p* value <1 and corrected-*p* value ≤1) (Table S4). As some sequences were assigned to more than one GO term, the total number of GO terms obtained in the dataset was much higher than the total number of the unique sequences. Approximately 12 significantly enriched pathways were obtained while the over-represented-*p* value <1 and corrected-*p* value <1 were set as the threshold (Table 2). Specifically, the following pathways were associated with GO terms related to binding, cofactor and coenzyme binding, redox processes (including oxidoreductase activity, oxidation reduction, peroxidase activity, response to oxidative stress, peroxidase reaction and oxidoreductase activity, acting on CH-OH donors, NAD or NADP as an acceptor), and organic acid-associated pathways containing carboxylic acid metabolism, glyoxylate cycle and fatty acid metabolism, within which two pathways significantly enriched with an "over-represented-*p* value of 0.0014394 and a corrected-*p* value of 0.50358" and an "over represented-*p* value of 0.052109 and corrected-*p* value of 1", respectively. And the last category was associated with transferase activity and transferring acyl groups, where acyl groups are converted into alkyl groups upon transfer.

Supplementary table related to this article can be found, in the online version, at http://dx.doi.org/10.1016/j.micres.2014.09.005.

KEGG analysis revealed that 105 enriched items were joined by 100 DEGs (*p*-value <1 and corrected *p*-value ≤1) (Table S5). Furthermore, with the threshold "*p*-value <1 and corrected *p*-value <1" significantly enriched, 7 significant enrichment items were obtained, including pathways associated with organic acid metabolic processes, for example, glyoxylate and dicarboxylate metabolism, pyruvate metabolism, tyrosine metabolism, cysteine and methionine metabolism, and other items, such as propanoate metabolism, microbial metabolism in diverse environments and carbon fixation pathways in prokaryotes (Table 3).

Supplementary table related to this article can be found, in the online version, at http://dx.doi.org/10.1016/j.micres.2014.09.005.

### 3.6. Validation of differentially expressed genes by qRT-PCR

To validate the sequencing results, 15 DEGs were selected for further analysis through qRT-PCR (Table S6). Although the log2.Fold_change values for the transcriptome sequencing results differed somewhat from the corresponding value obtained from

**Table 3**
Significantly enriched KEGG terms of DEGs with the threshold of *p*-value <1 and corrected-*p* value <1 from the comparison of Cd-free and Cd-stressed samples.

| Id | KEGG term | Corrected *p*-value | DEG item | BG item |
|---|---|---|---|---|
| ko00630 | Glyoxylate and dicarboxylate metabolism | 0.019376 | 10 | 40 |
| ko00640 | Propanoate metabolism | 0.023014 | 8 | 29 |
| ko00620 | Pyruvate metabolism | 0.114142 | 9 | 47 |
| ko01120 | Microbial metabolism in diverse environments | 0.402778 | 30 | 313 |
| ko00720 | Carbon fixation pathways in prokaryotes | 0.402778 | 4 | 15 |
| ko00350 | Tyrosine metabolism | 0.727564 | 9 | 69 |
| ko00270 | Cysteine and methionine metabolism | 0.867491 | 6 | 40 |

Corrected-*p* value: the *p* value after correction, the smaller corrected-*p* value indicated more significant gene differential expression. DEG item: the number of DEGs associated with the KEGG term. BG item: all known genes associated with the KEGG term.

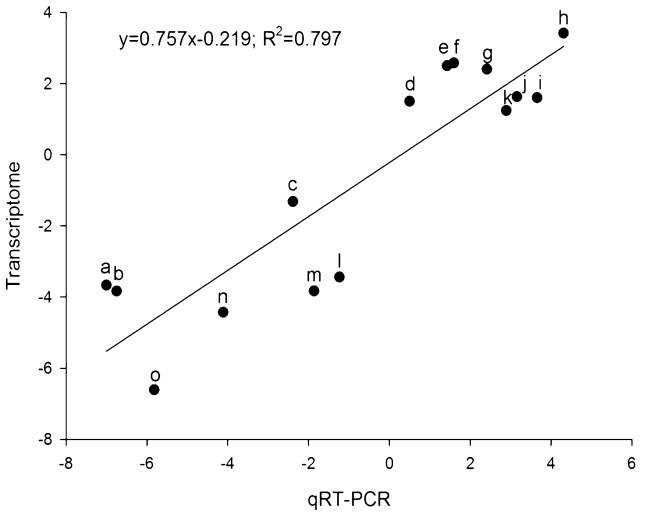


**Fig. 4.** Comparison of the log2.Fold_change values for the transcriptome sequencing results and qRT-PCR data of the 15 selected differentially expressed genes in *E. pisciphila* under Cd-free and Cd-stressed treatments. The lowercase letters represent the following unigenes: a: comp5493_c0; b: comp8159_c0; c: comp6365_c0; d: comp11606_c0; e: comp5960_c0; f: comp11611_c0; g: comp18838_c0; h: comp7406_c0; i: comp11798_c0; j: comp11825_c0; k: comp12237_c0; l: comp3367_c0; m: comp2997_c0; n: comp6001_c0; and o: comp10199_c0.

qRT-PCR, the regression of the RNA-seq and qRT-PCR data showed a good correlation ($R^2 = 0.797$) (Fig. 4).

Supplementary table related to this article can be found, in the online version, at http://dx.doi.org/10.1016/j.micres.2014.09.005.

## 4. Discussion

It has been suggested that suitable molecular tools are needed to develop fungal evolutionarily models more similar to HMs-exposed fungal taxa, such as mycorrhizal species (Hildebrandt et al. 2007; Pócsi 2011). Large-scale transcriptome sequencing is considered an effective technology to investigate initial molecular changes and complex pathways (Guo et al. 2011; Sun et al. 2013), and the accuracy of this technique has been confirmed in previous studies (Lagorce et al. 2012; Zhou et al. 2013b), consistent with the RNA-seq results obtained in the present study, confirmed through qRT-PCR. The present study primarily focused on the comparative transcriptional level analysis between Cd-free and Cd-stressed samples to estimate gene expression and gene networks in response to excessive Cd for *E. pisciphila*. The global molecular changes suggested 10 HMs tolerance pathways (Fig. 5), verified through GO and KEGG significant enrichment analyses. These results were consistent with the idea that the remarkable HMs tolerance mechanism for DSE fungi was exceedingly complex (Ban et al. 2012; Zhang et al. 2008). Herein, we investigated items typically involved in resistance to Cd toxicity.

Among the 575 identified DEGs, we detected 104 metal binding and 32 metal transport genes associated with HMs acquisition and homeostasis. Particularly, for bivalent metal cations, the major genes were involved with $Zn^{2+}$ binding, and the other genes were associated with $Fe^{2+}$, $Cu^{2+}$, $Mn^{2+}$, and $Ca^{2+}$ binding. In addition, we identified 3 MT genes, considered as a family of cysteine-rich polypeptides involved in intracellular Cd detoxification (Jacob et al. 2004; Pagani et al. 2012). Interestingly, the phytochelatin synthetase (PCS) unigenes, which encode phytochelatins (PCs) that contribute to HMs tolerance through binding intracellular metal ions, showed no changes in expression. In addition, a lack of PCs for most fungi was observed (Bellion et al. 2006; Cobbett 2000; Courbot et al. 2004). Generally, $Cd^{2+}$ entered cells through $Fe^{2+}$, $Ca^{2+}$ or $Zn^{2+}$ transporters (Wu et al. 2012), hence, the most effective mechanism for keeping toxic metals outside of cells is to eliminate the channels or transporters (Pócsi 2011). For example, the elimination of plasma membrane channels and transporters conferred metal tolerance to

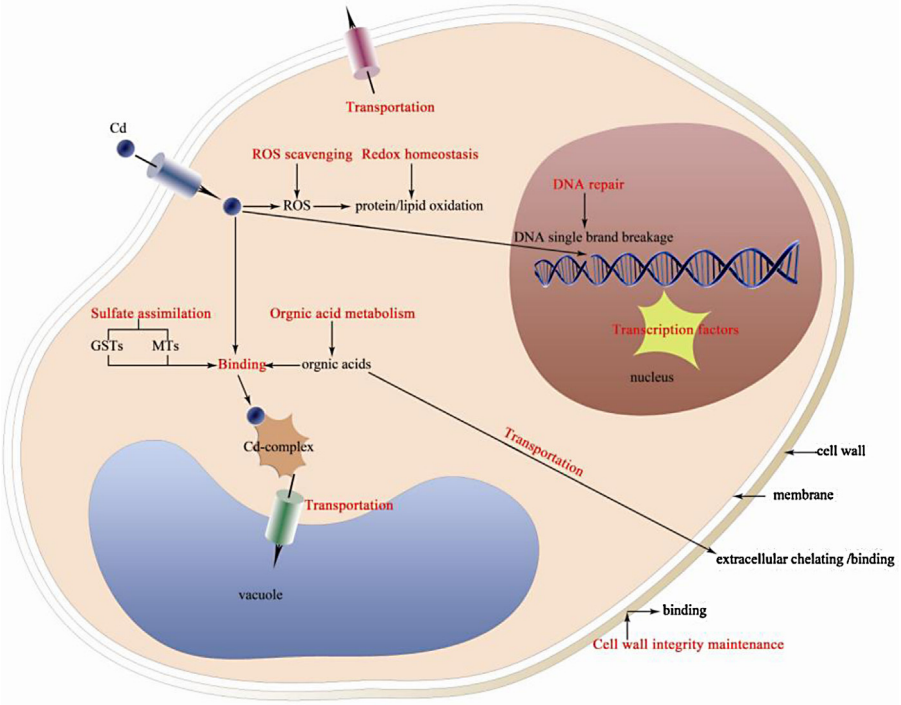


**Fig. 5.** Response of *E. pisciphila* to Cd detoxification, involving extracellular functions, such as extracellular metal ion binding and cell wall integrity maintenance, and intracellular processes, e.g., metal ion binding and transportation, organic acid metabolic processes, organic acid transportation, ROS scavenging, redox balance, transcription factor production, sulfate assimilation and DNA repair. The words shown in red indicate the characterized Cd tolerant pathways, which were described in the text. GSTs: glutathione S-transferases; MTs: metallothioneins; Cd: cadmium. (For interpretation of the references to color in this figure legend, the reader is referred to the web version of the article.)

metal-exposed *S. cerevisiae* (Wysocki and Tamás 2011). Expectedly, the results also showed that a majority of HMs transporters, such as $Zn^{2+}$ (Plaza et al. 2007; Talke et al. 2006), $Fe^{2+}$ and $Ca^{2+}$ transporters, were down-regulated, indicating a strategy for the inhibition of $Cd^{2+}$ passage through the membrane of *E. pisciphila*. Transporter proteins involved in metal tolerance facilitated the efflux of toxic metal ions from the cytosol or facilitated metal sequestration into intracellular compartments, such as vacuoles. Moreover, $K^+$ transporters were identified as $K^+$-specific membrane-bound transport proteins (Britto and Kronzucker 2008). The relationship between the regulation of these transporters and HMs tolerance remains controversial. However, it has recently been reported that the MthK contains a RCK (regulator of the conductance of $K^+$) domain, which binds divalent cations, such as $Cd^{2+}$ (Jiang et al. 2002). The KDC1 from carrot roots participates in the formation of heteromultimeric channels, which contribute to Cd tolerance after potentiation through external Cd (Picco et al. 2004). However, the lack of SynCaK increased resistance to zinc for cyanobacteria (Checchetto et al. 2013). Thus, up-modulated $K^+$ transporters are associated with Cd tolerance for *E. pisciphila*.

Typically, low-molecular weight compounds, such as amino and organic acids, act as important molecules, preventing the entry of metals into cells or by facilitating intracellular HMs detoxification through the chelation of various ligands (Lin and Aarts 2012; Rausch and Wachter 2005). Therefore, the biosynthesis, transport and metabolism of organic and amino acids are the central response to Cd exposure (Jin et al. 2008; Lin et al. 2013). Currently, 81 DEGs involved in organic and amino acid metabolism have been identified, similar to the transcriptome data of Cd-treated *Solanum nigrum* (Xu et al. 2012). Particularly, most genes were associated with down-regulated fatty acid biogenesis and up-regulated metabolism. Consistently, a relative decrease of fatty acids in arbuscular mycorrhizal fungi has been reported in zinc-polluted soil (Kelly et al. 1999). Unfortunately, the explanation for this response remains elusive.

Cd could induce the formation of ROS, leading to lipid peroxidation, enzyme inactivation and membrane damage, eventually resulting in an unbalanced cellular redox status. In defense against oxidative stresses, fungal oxidation is prevalent to remove oxygen radicals and repair oxidative damage through the biosynthesis of various antioxidants, such as GSH, especially SOD and CAT (Ban et al. 2012; Collin-Hansen et al. 2005; Zhang et al. 2008). In the present study, 12 GO significantly enriched pathways were identified, and 50% of these pathways were associated with redox processes, consistent with the elevation of redox pathways shown through the transcriptome analysis for other organisms (Lagorce et al. 2012; Lin et al. 2013; Xu et al. 2012), but lack of observations for fungi under Cd treatment. In fact, the obvious up-regulation of CAT, and Mn superoxide dismutase (SodB) genes was in consonance with our previous finding that the higher enzyme activities of SOD and CAT was positive correlated with the increasing Cd concentrations (Zhang et al. 2008). Nonetheless, there were some opposite reports on the Cd down-regulated expression of Mn-SOD such as *Pisum sativum* (Rodríguez-Serrano et al. 2009). For DEGs associated with POD, such as POD reaction, POD activity, L-ascorbate peroxidase 3, cytochrome c peroxidase (CcP), they were mainly down-regulated against Cd stress, indicating the little function of POD to ROS scavenging. The other up-regulated genes encoding for cell redox homeostasis and glutaredoxin (Bellion et al. 2006) also might confer redox balance. More than half of the unigenes involved in ROS scavenging and cell redox homeostasis were up-regulated, confirming the capacity of *E. pisciphila* to resist oxidative stress.

Notably, sulfate assimilation was a crucial process for the survival of living things after Cd exposure (Ernst et al. 2008; Joe et al. 2011; Lagorce et al. 2012; Lin et al. 2013). Under Cd stress, there might be a potential cytosolic mechanism for the synthesis of metal-induced specific sulfate-containing compounds, e.g., glutathione, cysteine, PCs, and MTs (Na and Salt 2011). The importance of the sulfur assimilation pathway in Cd-exposed *S. cerevisiae* was also emphasized in previous transcriptome data (Haugen et al. 2004). In the present study, approximately 75% of up-regulated genes in this pathway indicated roles of sulfate assimilation for Cd tolerance in *E. pisciphila*. For example, the GST gene, encoding a ubiquitous family of multifunctional enzymes, showed the largest log2.Fold_change (4.8056), demonstrating significance in the promotion of Cd tolerance (Villiers et al. 2011).

Typically, the integral cell wall is considered the initial barrier to metal entrance through chelation, binding and accumulation of metals (Colzi et al. 2011; Ruotolo et al. 2008). Thus, any degradation leading to the damage of the cell wall integrity would also reduce metal tolerance. Fungal cell wall components, such as cellulose, semi-cellulose, melanin and chitin, typically function in metal ion biosorption (Ban et al. 2012; Zhang et al. 2008). However, HMs, such as Mn, Hg, Ag, Pb, As and Cd, lead to cell wall damage through increased chitinase expression (van Keulen et al. 2008). Studies have shown that chitinase was up-regulation under Cd stress (Békésiová et al. 2008; Metwally et al. 2005; Rodríguez-Serrano et al. 2009); particularly, the significant up-regulation of chitinase was observed during fungal autolysis (Baratto et al. 2006). However, four chitinase genes were surprisingly down-regulated in *E. pisciphila*. Thus, it is reasonable that the down-regulated chitinase might not result in the degradation of cell wall components, such as chitin, thereby maintaining the cell wall integrity when *E. pisciphila* is challenged with Cd. Besides, direct evidence on *Gaeumannomyces cylindrosporus* (one typical DSE fungi) supported a decrease in Cd toxicity, associated with an increase in the available carbon sources (Ban et al. 2012). The KEGG analysis revealed significantly enriched carbon fixation pathways that likely contribute to the accumulation of cell wall components, similar to Cd-stressed *S. cerevisiae* (Thorsen et al. 2009). It has been suggested that the decreasing degradation and increasing biogenesis of cell wall constituents might contribute to Cd tolerance in *E. pisciphila*, consistent with the thickening of the cell wall after exposure to toxic $Cd^{2+}$ (Zhang et al. 2008).

Metal-responsive TFs play a role in metal homeostasis, acting as molecular switches for gene expression, for instance, stimulating the expression of antioxidant enzymes (Hosiner et al. 2009), and the removal and degradation of proteins (Medicherla and Goldberg 2008; Thorsen et al. 2009). In lower eukaryotes, TFs contain regulatory cysteine clusters with different amino acid sequences, serving diverse functions (Günther et al. 2012) that typically do not function independently of each other (Salin et al. 2008). The results showed that 50 DEGs were associated with various TFs. Although only a half of the TFs were up-regulated, a large number of Cd-triggered TFs exerted unpredictable effects on HMs tolerance in *E. pisciphila*. In addition, Cd exposure could induce single-strand breakage in DNA and produce genotoxic and mutagenic events through the inhibition of various DNA repair processes, particularly, base excision and mismatch repair (Giaginis et al. 2006). Therefore, ubiquitous repair genes play a crucial role in organisms challenged with Cd, such as bacteria (Lagorce et al. 2012; Sandigursky and Franklin 2000) and fungi (Ruotolo et al. 2008; Serero et al. 2008). In the present study, 80% of the DNA repair genes were markedly up-regulated, manifesting positive influences in conferring Cd-tolerance in *E. pisciphila*.

## 5. Conclusions

This study was the first comprehensive transcriptome analysis of a DSE under Cd stress based on RNA-seq data. Importantly, 228 unigenes associated with Cd-tolerance were identified among

575 DEGs. We highlighted the molecular mechanism associated with a combination of at least 10 HMs-tolerance pathways for Cd adaptation in *E. pisciphila*. Thus, the RNA-seq data suggested that acclimatization to Cd stress, in *E. pisciphila*, is accomplished through complex and diverse mechanisms, even involving multiple complex physiological and metabolic pathways.

## Acknowledgments

The authors would like to thank Miss Qin Qiao from the School of Agriculture, Yunnan University, Miss Shan Xiao from the Majorbio Company and Mr. Zhen Sun from Novagene company for assistance in preparing this manuscript. Thank Mr. Joshua Smith (The University of British Columbia, Canada) very much for his great editing job on the manuscript. This research was financially supported by the National Natural Science Foundation of China (31160009; 41161083; 31460114; 41461073), the Key Project of Applied Basic Research of Yunnan (2013FA001), the Postdoctoral Sustentation Fund supported through Yunnan University and Young Academic and Technical Leader Raising Foundation of Yunnan Province (2012HB006).

## References

Anders S, Huber W. Differential expression analysis for sequence count data. Genome Biol 2011;11:R106.
Békésiová B, Hraška Š, Libantová J, Moravčíková J, Matušíková I. Heavy-metal stress induced accumulation of chitinase isoforms in plants. Mol Biol Rep 2008;35:579–88.
Ban Y, Tang M, Chen H, Xu Z, Zhang H, Yang Y. The response of dark septate endophytes (DSE) to heavy metals in pure culture. PLOS ONE 2012;7:e47968.
Baratto CM, Dutra V, Boldo JT, Leiria LB, Vainstein MH, Schrank A. Isolation, characterization, and transcriptional analysis of the chitinase chi2 gene (DQ011663) from the biocontrol fungus *Metarhizium anisopliae* var. anisopliae. Curr Microbiol 2006;53:217–21.
Bellion M, Courbot M, Jacob C, Blaudez D, Chalot M. Extracellular and cellular mechanisms sustaining metal tolerance in ectomycorrhizal fungi. FEMS Microbiol Lett 2006;254:173–81.
Bertin G, Averbeck D. Cadmium: cellular effects, modifications of biomolecules, modulation of DNA repair and genotoxic consequences (a review). Biochimie 2006;88:1549–59.
Britto DT, Kronzucker HJ. Cellular mechanisms of potassium transport in plants. Physiol Plant 2008;133:637–50.
Checchetto V, Formentin E, Carraretto L, Segalla A, Giacometti GM, Szabo I, et al. Functional characterization and determination of the physiological role of a calcium-dependent potassium channel from cyanobacteria. Plant Physiol 2013;162:953–64.
Cobbett CS. Phytochelatins and their roles in heavy metal detoxification. Plant Physiol 2000;123:825–32.
Collin-Hansen C, Andersen RA, Steinnes E. Molecular defense systems are expressed in the king bolete (*Boletus edulis*) growing near metal smelters. Mycologia 2005;97:973–83.
Colzi I, Doumett S, Del Bubba M, Fornaini J, Arnetoli M, Gabbrielli R, et al. On the role of the cell wall in the phenomenon of copper tolerance in *Silene paradoxa* L. Environ Exp Bot 2011;72:77–83.
Courbot M, Diez L, Ruotolo R, Chalot M, Leroy P. Cadmium-responsive thiols in the ectomycorrhizal fungus *Paxillus involutus*. Appl Environ Microbiol 2004;70:7413–7.
Deram A, Languereau-Leman F, Howsam M, Petit D, Haluwyn CV. Seasonal patterns of cadmium accumulation in *Arrhenatherum elatius* (Poaceae): influence of mycorrhizal and endophytic fungal colonisation. Soil Biol Biochem 2008;40:845–8.
Diao YH, Li T, Zhao ZW. Zinc accumulation characteristics of two *Exophiala* strains and their antioxidant response to $Zn^{2+}$ stress. J Environ Prot 2013;4:12–9.
Ernst WH, Krauss GJ, Verkleij JA, Wesenberg D. Interaction of heavy metals with the sulphur metabolism in angiosperms from an ecological point of view. Plant Cell Environ 2008;31:123–43.
Günther V, Davis AM, Georgiev O, Schaffner W. A conserved cysteine cluster, essential for transcriptional activity, mediates homodimerization of human metal-responsive transcription factor-1 (MTF-1). BBA Mol Cell Res 2012;1823:476–83.
Giaginis C, Gatzidou E, Theocharis S. DNA repair systems as targets of cadmium toxicity. Toxicol Appl Pharmacol 2006;213:282–90.
Grabherr MG, Haas BJ, Yassour M, Levin JZ, Thompson DA, Amit I, et al. Full-length transcriptome assembly from RNA-Seq data without a reference genome. Nat Biotechnol 2011;29:644–52.
Guo S, Zheng Y, Joung JG, Liu S, Zhang Z, Crasta OR, et al. Transcriptome sequencing and comparative analysis of cucumber flowers with different sex types. BMC Genomics 2011;11:384.
Haugen AC, Kelley R, Collins JB, Tucker CJ, Deng C, Afshari CA, et al. Integrating phenotypic and expression profiles to map arsenic-response networks. Genome Biol 2004;5:R95.
Hildebrandt U, Regvar M, Bothe H. Arbuscular mycorrhiza and heavy metal tolerance. Phytochemistry 2007;68:139–46.
Hosiner D, Lempiäinen H, Reiter W, Urban J, Loewith R, Ammerer G, et al. Arsenic toxicity to *Saccharomyces cerevisiae* is a consequence of inhibition of the TORC1 kinase combined with a chronic stress response. Mol Biol Cell 2009;20:1048–57.
Jacob C, Courbot M, Martin F, Brun A, Chalot M. Transcriptomic responses to cadmium in the ectomycorrhizal fungus *Paxillus involutus*. FEBS Lett 2004;576:423–7.
Jiang Y, Lee A, Chen J, Cadene M, Chait BT, MacKinnon R. Crystal structure and mechanism of a calcium-gated potassium channel. Nature 2002;417:515–22.
Jin YH, Dunlap PE, McBride SJ, Al-Refai H, Bushel PR, Freedman JH. Global transcriptome and deletome profiles of yeast exposed to transition metals. PLoS Genet 2008;4:e1000053.
Joe MH, Im SH, Song HP, Kim DH. Genome-wide response of *Deinococcus radiodurans* on cadmium toxicity. J Microbiol Biotechnol 2011;21:438–47.
Kelly J, Häggblom M, Tate R. Changes in soil microbial communities over time resulting from one time application of zinc: a laboratory microcosm study. Soil Biol Biochem 1999;31:1455–65.
Lagorce A, Fourçans A, Dutertre M, Bouyssiere B, Zivanovic Y, Confalonieri F. Genome-wide transcriptional response of the archaeon *Thermococcus gammatolerans* to cadmium. PLOS ONE 2012;7:e41935.
Li B, Dewey C. RSEM: accurate transcript quantification from RNA-Seq data with or without a reference genome. BMC Bioinf 2011;12:323.
Li T, Liu M, Zhang X, Zhang H, Sha T, Zhao Z. Improved tolerance of maize (*Zea mays* L.) to heavy metals by colonization of a dark septate endophyte (DSE) *Exophiala pisciphila*. Sci Total Environ 2011;409:1069–74.
Lin CY, Trinh NN, Fu SF, Hsiung YC, Chia LC, Lin CW, et al. Comparison of early transcriptome responses to copper and cadmium in rice roots. Plant Mol Biol 2013;81:1–16.
Lin YF, Aarts MG. The molecular mechanism of zinc and cadmium stress response in plants. Cell Mol Life Sci 2012;69:3187–206.
Mao X, Cai T, Olyarchuk JG, Wei L. Automated genome annotation and pathway identification using the KEGG Orthology (KO) as a controlled vocabulary. Bioinformatics 2005;21:3787–93.
Medicherla B, Goldberg AL. Heat shock and oxygen radicals stimulate ubiquitin-dependent degradation mainly of newly synthesized proteins. J Cell Biol 2008;182:663–73.
Metwally A, Safronova VI, Belimov AA, Dietz KJ. Genotypic variation of the response to cadmium toxicity in *Pisum sativum* L. J Exp Bot 2005;56:167–78.
Mortazavi A, Williams BA, McCue K, Schaeffer L, Wold B. Mapping and quantifying mammalian transcriptomes by RNA-Seq. Nat Methods 2008;5:621–8.
Na G, Salt DE. The role of sulfur assimilation and sulfur-containing compounds in trace element homeostasis in plants. Environ Exp Bot 2011;72:18–25.
Newsham KK, Upson R, Read DJ. Mycorrhizas and dark septate root endophytes in polar regions. Fungal Ecol 2009;2:10–20.
Nota B, Verweij RA, Molenaar D, Ylstra B, van Straalen NM, Roelofs D. Gene expression analysis reveals a gene set discriminatory to different metals in soil. Toxicol Sci 2010;115:34–40.
Novais SC, De Coen W, Amorim MJ. Transcriptional responses in *Enchytraeus albidus* (Oligochaeta): comparison between cadmium and zinc exposure and linkage to reproduction effects. Environ Toxicol Chem 2012;31:2289–99.
Pócsi I. Toxic metal/metalloid tolerance in fungi—a biotechnology-oriented approach. In: Banfalvi G, editor. Cellular effects of heavy metals. New York: Springer; 2011. p. 31–58.
Pagani MA, Tomas M, Carrillo J, Bofill R, Capdevila M, Atrian S, et al. The response of the different soybean metallothionein isoforms to cadmium intoxication. J Inorg Biochem 2012;117:306–15.
Picco C, Bregante M, Naso A, Gavazzo P, Costa A, Formentin E, et al. Histidines are responsible for zinc potentiation of the current in KDC1 carrot channels. Biophys J 2004;86:224–34.
Plaza S, Tearall KL, Zhao FJ, Buchner P, McGrath SP, Hawkesford MJ. Expression and functional analysis of metal transporter genes in two contrasting ecotypes of the hyperaccumulator *Thlaspi caerulescens*. J Exp Bot 2007;58:1717–28.
Rausch T, Wachter A. Sulfur metabolism: a versatile platform for launching defence operations. Trends Plant Sci 2005;10:503–9.
Regvar M, Likar M, Piltaver A, Kugonič N, Smith JE. Fungal community structure under goat willows (*Salix caprea* L.) growing at metal polluted site: the potential of screening in a model phytostabilisation study. Plant Soil 2011;330:345–56.
Rodríguez-Serrano M, Romero-Puertas MC, Pazmiño DM, Testillano PS, Risueño MC, Luis A, et al. Cellular response of pea plants to cadmium toxicity: cross talk between reactive oxygen species, nitric oxide, and calcium. Plant Physiol 2009;150:229–43.
Ruotolo R, Marchini G, Ottonello S. Membrane transporters and protein traffic networks differentially affecting metal tolerance: a genomic phenotyping study in yeast. Genome Biol 2008;9:R67.
Ruotsalainen AL, Markkola A, Kozlov MV. Root fungal colonisation in *Deschampsia flexuosa*: effects of pollution and neighbouring trees. Environ Pollut 2007;147:723–8.
Salin H, Fardeau V, Piccini E, Lelandais G, Tanty V, Lemoine S, et al. Structure and properties of transcriptional networks driving selenite stress response in yeasts. BMC Genomics 2008;9:333.

Sandigursky M, Franklin WA. Uracil-DNA glycosylase in the extreme thermophile *Archaeoglobus fulgidus*. J Biol Chem 2000;275:19146–9.
Serero A, Lopes J, Nicolas A, Boiteux S. Yeast genes involved in cadmium tolerance: identification of DNA replication as a target of cadmium toxicity. DNA Repair 2008;7:1262–75.
Storey JD, Tibshirani R. Statistical significance for genomewide studies. Proc Natl Acad Sci USA 2003;100:9440–5.
Sun Y, Wang F, Wang N, Dong Y, Liu Q, Zhao L, et al. Transcriptome exploration in *Leymus chinensis* under saline-alkaline treatment using 454 pyrosequencing. PLOS ONE 2013;8:e53632.
Talke IN, Hanikenne M, Krämer U. Zinc-dependent global transcriptional control, transcriptional deregulation, and higher gene copy number for genes in metal homeostasis of the hyperaccumulator *Arabidopsis halleri*. Plant Physiol 2006;142:148–67.
Thorsen M, Perrone G, Kristiansson E, Traini M, Ye T, Dawes I, et al. Genetic basis of arsenite and cadmium tolerance in *Saccharomyces cerevisiae*. BMC Genomics 2009;10:105.
van Keulen H, Wei R, Cutright TJ. Arsenate-induced expression of a class III chitinase in the dwarf sunflower *Helianthus annuus*. Environ Exp Bot 2008;63:281–8.
Villiers F, Ducruix C, Hugouvieux V, Jarno N, Ezan E, Garin J, et al. Investigating the plant response to cadmium exposure by proteomic and metabolomic approaches. Proteomics 2011;11:1650–63.
Winer J, Jung CKS, Shackel I, Williams PM. Development and validation of real-time quantitative reverse transcriptase–polymerase chain reaction for monitoring gene expression in cardiac myocytes *in vitro*. Anal Biochem 1999;270:41–9.
Wu H, Chen C, Du J, Liu H, Cui Y, Zhang Y, et al. Co-overexpression FIT with AtbHLH38 or AtbHLH39 in *Arabidopsis*-enhanced cadmium tolerance via increased cadmium sequestration in roots and improved iron homeostasis of shoots. Plant Physiol 2012;158:790–800.
Wysocki R, Tamás MJ. How *Saccharomyces cerevisiae* copes with toxic metals and metalloids. FEMS Microbiol Rev 2011;34:925–51.
Xu J, Sun J, Du L, Liu X. Comparative transcriptome analysis of cadmium responses in *Solanum nigrum* and *Solanum torvum*. New Phytol 2012;196:110–24.
Young MD, Wakefield MJ, Smyth GK, Oshlack A. Gene ontology analysis for RNA-seq: accounting for selection bias. Genome Biol 2011;11:R14.
Zhan FD. [Dissertation] Study on the tolerance mechanisms of *Exophila pisciphilia* ACCC32496 for cadmium [Dissertation]. Yunnan University; 2012.
Zhan F, He Y, Zu Y, Li T, Zhao Z. Characterization of melanin isolated from a dark septate endophyte (DSE), *Exophiala pisciphila*. World J Microbiol Biotechnol 2011;27:2483–9.
Zhang Y, Zhang Y, Liu M, Shi X, Zhao Z. Dark septate endophyte (DSE) fungi isolated from metal polluted soils: their taxonomic position, tolerance, and accumulation of heavy metals in vitro. J Microbiol 2008;46:624–32.
Zhou WW, Liang QM, Xu Y, Gurr GM, Bao YY, Zhou XP, et al. Genomic insights into the glutathione S-transferase gene family of two rice planthoppers, *Nilaparvata lugens* (Stål) and *Sogatella furcifera* (Horváth) (Hemiptera: Delphacidae). PLOS ONE 2013a;8:e56604.
Zhou ZS, Yang SN, Li H, Zhu CC, Liu ZP, Yang ZM. Molecular dissection of mercury-responsive transcriptome and sense/antisense genes in *Medicago truncatula* by high-throughput sequencing. J Hazard Mater 2013b;252–253:123–31.
Zhu B, Liu L, Li DL, Ling F, Wang GX. Developmental toxicity in rare minnow (*Gobiocypris rarus*) embryos exposed to Cu, Zn and Cd. Ecotoxicol Environ Saf 2014;104:269–77.